Int J Adv Manuf Technol (2017) 91:3799–3806
DOI 10.1007/s00170-017-0050-6

ORIGINAL ARTICLE

Fabrication of freeform progressive addition lenses using a self-developed long stroke fast tool servo

Haihua Feng[1,2] · **Risheng Xia**[1] · **Yiyu Li**[1,2] · **Jiaojie Chen**[1,2] · **Yimin Yuan**[1,2] · **Dexi Zhu**[1,2] · **Siyun Chen**[1,2] · **Hao Chen**[1,2]

Received: 3 June 2016 / Accepted: 16 January 2017 / Published online: 30 January 2017

Abstract A long stroke fast tool servo (LFTS) system with a maximum stroke range of ±4 mm based on the voice coil actuator was developed and integrated on a diamond turning machine (DTM) for the fabrication of freeform progressive addition lenses (PALs). The LFTS utilized a three-ring cascade control system for the motion trajectory control of a diamond tool. The numerical control codes of the tool path were transferred from the 3D surface data with freeform features. The complete process chain from tool path generation and diamond machining to power measurement was experimentally demonstrated. The obtained surface form accuracy was 6.7 μm (rms), and the measured power of the PAL agreed well with the theoretical design indicating the desirable processing capability of LFTS for the customized freeform spectacle optics.

Keywords Freeform · Diamond turning · Fast tool servo · Progressive addition lens

1 Introduction

Ophthalmic progressive addition lenses (PALs) are used in clinics to correct presbyopia [1] in older patients and control the progression of myopia in schoolchildren. The PAL consists of a distant zone, a near zone and a corridor zone between the distant and near zones, which is achieved by continuously changing the radius of curvature on the surface that can be treated as freeform geometry. As a result, the surface power varies progressively from a minimum value at the distant zone to a maximum value at the near zone providing the required addition for near vision. The traditional and cost-effective injection molding method has been used for massive production of PALs. Both the glass mold [2, 3] produced by grinding process and the aluminum alloy mold [4, 5] or copper mold [6, 7] produced by single-point diamond turning with slow tool servo (STS) have been introduced. However, the injection-molded PALs suffer from refractive index variation and geometric deformation due to the rheological properties of polymers leading to the distortion and deviation of optical performance for vision correction. Nowadays, when personalized PALs have become fashionable, the customized designs are required for the lightweight, functional, and adaptable PAL of each patient. Because of the great variety of customized design philosophies and the relatively low production rate of STS due to the limitation on slide speed, the diamond turning method with fast tool servo (FTS) becomes the best choice for direct fabrication of personalized PALs.

FTS supported by either a piezo actuator or a voice coil actuator has been used for the manufacture of freeform optical elements [8–14]. Piezo-driven systems, offering the advantages of higher peak acceleration and bandwidth, are limited in the travel of several hundred microns, therefore unable to deal with the asymmetric features usually measured about 2 mm in magnitude in freeform PALs. Voice-coil-driven system is considered as the prime candidate for the long stroke fast tool servo (LFTS). However, the application of LFTS in PAL fabrication and the technical details of LFTS development have not yet been discussed in literatures before. In this study, a LFTS based on voice coil actuator was developed and integrated on a diamond turning machine (DTM) for surface machining of freeform PALs. The paper was organized as

✉ Yiyu Li
liyiyu2008@gmail.com

[1] School of Optometry and Ophthalmology, Wenzhou Medical University, Wenzhou, China

[2] The Eye Hospital, Wenzhou Medical University, Wenzhou, China

follows. The mechanical structure and the control system of LFTS were introduced in "LFTS" section. The generation of tool path for freeform machining of the PAL was investigated in "Tool path for surface machining" section and used for the experiment of the PAL fabrication demonstrated in "Freeform machining of PAL" section. The measurement of the geometry and the optical characteristics of PAL were carried out in "Results of freeform machining" section.

2 LFTS

2.1 Structure design of LFTS

For precision manufacture of freeform PALs, a DTM with an additional LFTS was developed as shown in Fig. 1. The DTM comprises four parts: a C-axis aerostatic spindle to rotate the workpiece, an X-axis precise linear servo based on a rolling guide to move the spindle laterally, a Z-axis LFTS with maximum stroke of ±4 mm and maximum acceleration of 370 ms^{-2} based on a voice coil actuator (TMEC0950-025, Kunshan Tongmao Electronics), and a milling arbor driving the milling tool for lens cribbing process.

The motion of diamond tools which is connected to the tool bar/slider is controlled by LFTS as shown in Fig. 2. The position feedback sensor (Renishaw grating ruler) with a theoretical resolution of 1.2 nm operates in a closed control loop with the voice coil actuator to control the forward and reverse motion of the diamond tool in real time. Meanwhile, the stroke of the diamond tool is synchronized with the encoder outputs of the workpiece spindle and the X-axis linear servo to guarantee the machining process for the asymmetric freeform surface.

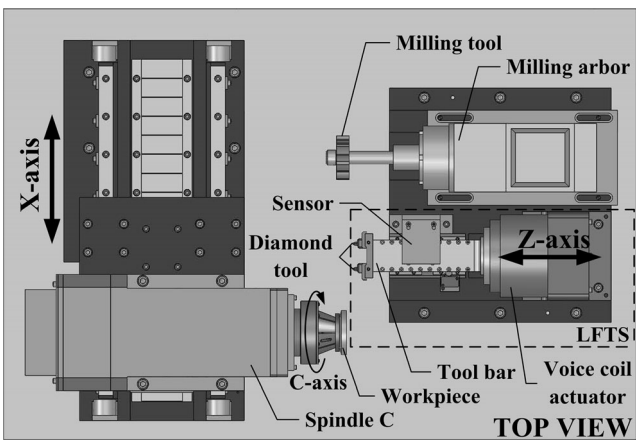

Fig. 1 The structure layout of the T-base DTM with LFTS for surface machining of PAL

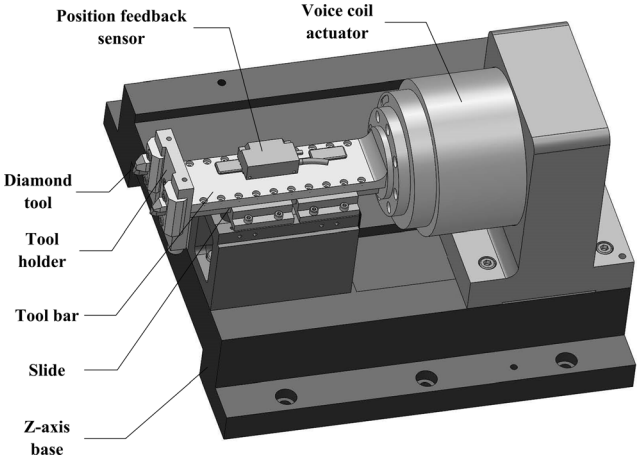

Fig. 2 The structure layout of LFTS system

2.2 Control of LFTS

To generate the correct driving voltage of voice coil actuator for the motion control of the diamond tool, a closed loop control system including the position loop, the velocity loop, and the current loop was employed to achieve the three-ring cascade control of LFTS as shown in Fig.3. The system acquires the actual positions of the diamond tool which are measured by the linear displacement detection device and then compares them both with the reference displacement signals and the reference velocity signals given in advance to derive the position deviation and velocity deviation, respectively.

The position controller consists of PI controller, "prediction" feed forward, displacement sensor, and signal processing circuit. The PI controller, containing the proportional element and the integral element, was combined with "prediction" feed forward to generate the input signal for the velocity controller. The proportional element with the proportional gain was used to realize the balance between the lag errors and the rigidity of the control loop. The integral element with the integral action time was employed to compensate for the stationary disturbance.

The velocity controller comprises velocity filter, PI controller, displacement sensor, and signal processing circuit. The actual velocity provided by the velocity filter was calculated based on the actual displacement. Then it was compared with the input reference velocity signal to generate the velocity deviation which was followed by the process of the PI controller and then combined with the feed forward signal to determine the input signal for the current controller.

For the current controller, the current filter containing a notch filter and a torque limiter can guarantee a reasonable current for the voice coil actuator and meanwhile prevent overcurrent. The control signal can be magnified by the power driver part to drive the actuator.

The control system was operated in the B&R Automation Studio integrated development environment and B&R

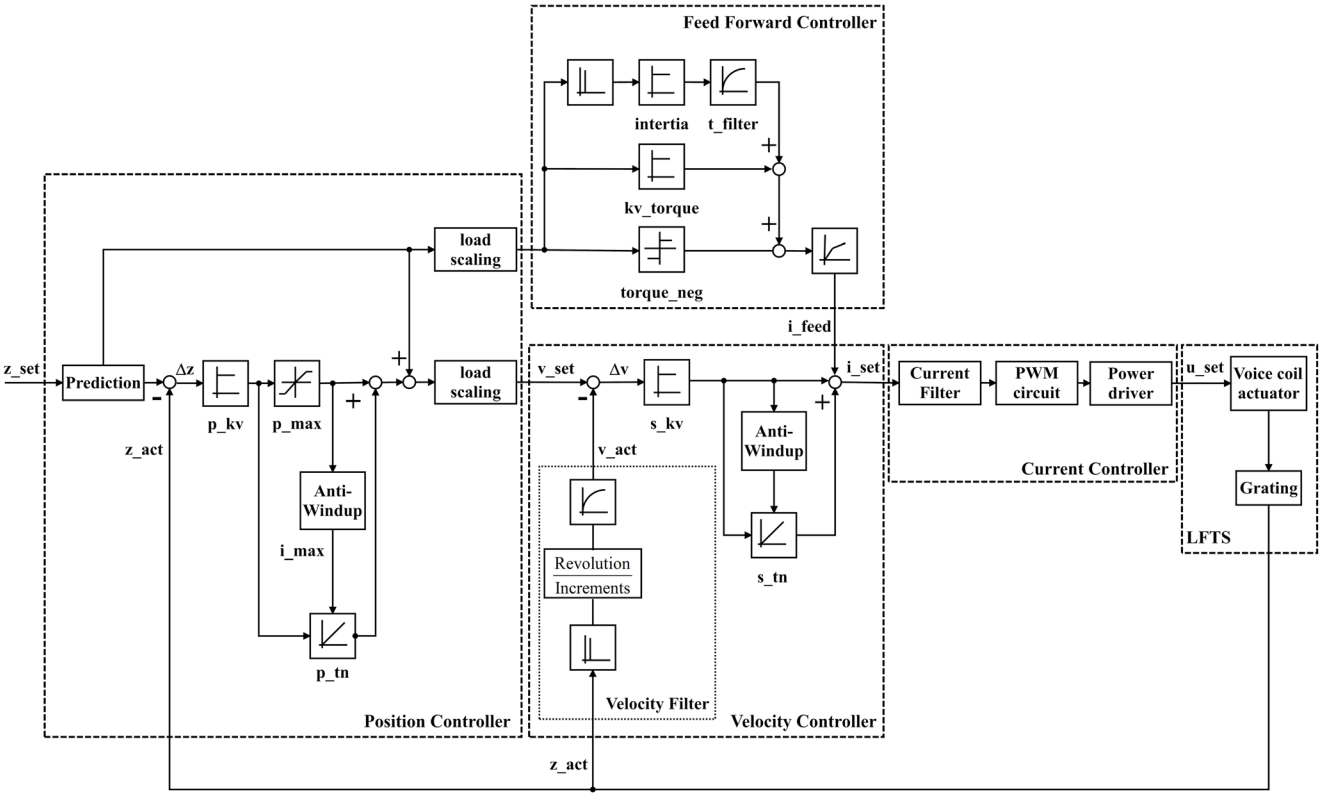

Fig. 3 Block diagram of the closed loop control of LFTS

Programming Computer Controller (PCC) with the values of the key parameters shown in Table 1 for the desirable system performance in practice.

2.3 Tracking performance in sinusoidal motion

The performance of LFTS working in air-cut condition was first evaluated by tracking a series of sinusoidal motions of various amplitudes and frequencies. The response of LFTS was recorded and compared with the command to derive the tracking errors as shown in Fig. 4. For a fixed working frequency, the RMS tracking error increased almost linearly with the increment of amplitude. Higher frequency could also worsen tracking errors. Figure 5 shows a part of the recorded LFTS response to the command of a sinusoidal motion. The actual trajectory of the diamond tool controlled by LFTS appeared to match the command very well except for the maximum tracking error of about 13 μm that happened at the rising edge and the trailing edge where the decelerated motion took place leading to the overall tracking errors of about 8 μm (rms).

The surface finish of the PAL typically requires the shape error of less than 12 μm (rms). Therefore, to guarantee the surface form accuracy, the working frequency of LFTS can reach 30 Hz with the amplitude of 1.0 mm. This dynamic range can cover the asymmetric variation of the freeform surface in most PALs. As the variation of surface elevation decreases within a smaller lens aperture especially when prism thinning method [15] is utilized for the PAL design, higher working frequency of LFTS could be employed for machining the interior area of the surface to improve the processing efficiency.

Table 1 The important parameters for the control system of LFTS

Parameters	Value	Unit	Description
p_kv	600	1/s	Proportional amplification in position controller
p_tn	0.0004	s	Integral action time in position controller
t_predict	0.0008	s	Prediction time
p_max	1e + 030	Units/s	Maximum proportional action
i_max	1e + 030	Units/s	Maximum integral action
s_kv	0.15	Asec/rev	Proportional amplification in velocity controller
s_tn	0.15	s	Integral action time in velocity controller

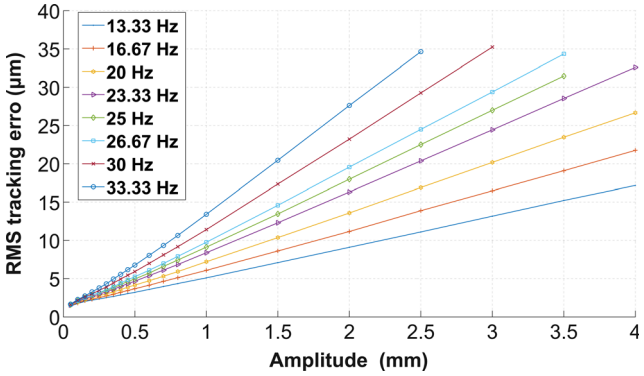

Fig. 4 The RMS tracking error of LFTS following the sinusoidal motion of different amplitudes and frequencies in air-cut conditions

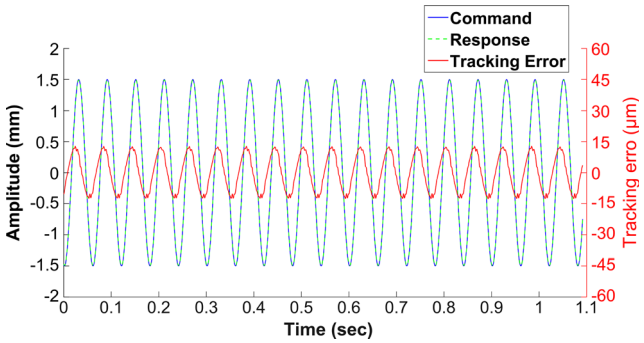

Fig. 5 The recorded response of LFTS tracking a sinusoidal motion with 1.5 mm amplitudes and frequency of 16.67 Hz

3 Tool path for surface machining

3.1 Freeform design of PAL

The design methods of PALs can be divided into two categories, direct methods and indirect methods. Here, a self-developed software based on the direct design method proposed by Winthrop [16, 17] was used for the customized design of PALs. The front convex surface of the PAL was chosen to be a sphere with constant curvature; so, the progressive change of the optical power was achieved by smoothly changing the curvature of the rear surface. The optical power of the rear surface was first assigned along the meridian line on the lens. Then, the surface was generated from the meridian line by prescribing curves which were transverse to it. The shapes of these curves were chosen to have the desired surface curvatures on the meridian line.

Figure 6 shows the surface-based spherical power and cylinder of the PAL designed for a distant correction of −1.85 diopter with an add power of 2.00 diopter. The corridor is 14 mm measured from the geometric center to the nominal add-power position. The designed rear surface of the PAL is shown in Fig. 7. The performance of the PAL in vision correction can be furtherly simulated by ray tracing of the complete PAL in front of a model eye, offering a marked improvement over the surface analysis. However, the discussion of visual correction is not included in this letter which focuses on the manufacture issue.

3.2 Tool path generation

To process the coordinate data of the PAL surface into an appropriate format for machining, a proprietary software using Matlab programming was developed. The software calculated the profile in at least 4.7×10^5 supporting points in a polar mesh to transfer the 3D surface data with the freeform features into the numerical code. The point elements were equally spaced with an incremental size of 25 μm along the radial direction and with a circumferential spacing of 0.4 mm. So, the point spacing in the angular direction depends on the fixed circumferential spacing and the radial position of the tool node. Therefore, the point density decreased when the tool node approached the lens center. Once the angular spacing became smaller than the threshold of 2°, the method of equal angular spacing was adopted to rule the sampling to maintain the point density.

The required tool path for freeform machining of the PAL followed a spiral trajectory as shown in Fig.7 where the feed

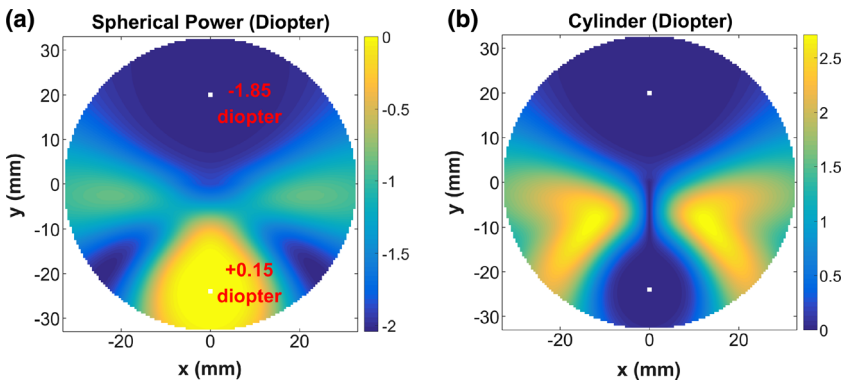

Fig. 6 The calculated power maps of the designed PAL (add power of 2.00 diopter). **a** Spherical power and **b** cylinder

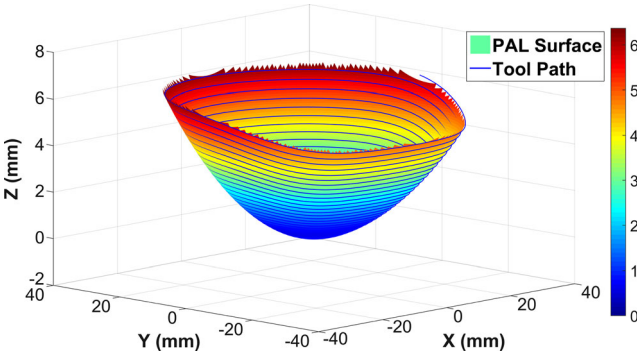

Fig. 7 The designed freeform surface of the PAL combined with the corresponding tool path for diamond turning. The feed rate in radial direction was 1 mm per revolution just for demonstration

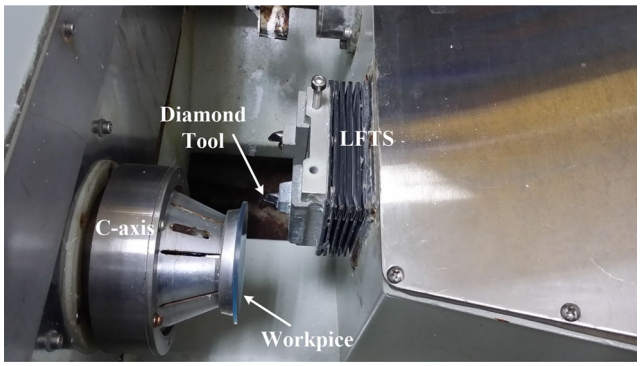

Fig. 8 Diamond turning of the PAL with LFTS mounted on the DTM

rate was set to be 1 mm per revolution just for demonstration. Typically in diamond turning applications, the tool radius compensation is done in the normal direction [18]. However, in this study, the radius of the tool tip is much smaller than the local radius of the freeform surface which also possesses a relative flat slope along the radial directions. So, the tool radius compensation only accounts for a tiny change normally less than 0.025 diopter of the local surface power and therefore has little effect on vision correction and can be neglected.

4 Freeform machining of PAL

Since the freeform surface was designed for the rear surface of the PAL, a semi-finished CR-39 blank lens with a prefabricated front spherical surface was chosen as the workpiece to be held by a pneumatic chuck on the aerostatic spindle as shown in Fig. 8. The milling tool was first used for the cribbing process to obtain the required lens size. Then, diamond turning was conducted to generate the freeform surface. For rough cutting, a polycrystalline diamond tool was employed with a cutting depth of 0.5 mm. For finish cutting, a natural diamond tool was used with a cutting depth of 0.1 mm. The machining time of rough cutting and finish cutting was about 50 and 90 s, respectively. The required total stroke of LFTS was ±1.3 mm. According to the tracking error shown in Fig. 4 and meanwhile considering the required shape error of the PAL surface, the nominal working frequency of 30 Hz could be chosen for LFTS. To achieve a reasonable smooth surface with slight diamond turning marks, the feed per revolution for finish cutting was 25 μm.

The required motion of the diamond tool was plotted with respect to the processing time as shown in Fig. 9. The spindle speed was set to be 1000 rpm leading to the nominal working frequency of 33.3 Hz for LFTS. The motion amplitude decreased gradually and nonlinearly during the machining process. The inset map in Fig. 9 demonstrates that the required trajectory of the tool does not follow an exact sinusoidal motion but an approximate rectangular one.

The response signals of LFTS were recorded during machining process and shown in Fig. 10a for the evaluation of tracking performance in position control. Due to the limited memory space allocated for motion monitor in control system, the response signals composed of 2730 sampling data within 0.82 s were stored for the periphery zone of the surface. The tracking error leading to the shape error of the local surface was derived by comparing the response signals with the command. Then, the fast Fourier transform method was used to

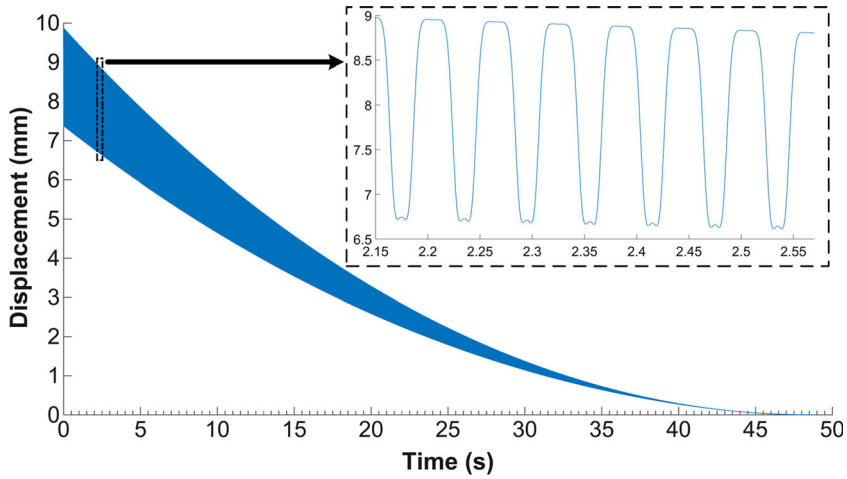

Fig. 9 The required motion trajectory of the diamond tool for freeform surface machining of the designed PAL. The spindle speed was set to be 1000 rpm. The *inset map* zooms in on the motion trajectory within 0.42 s corresponding to the seven revolutions of the spindle

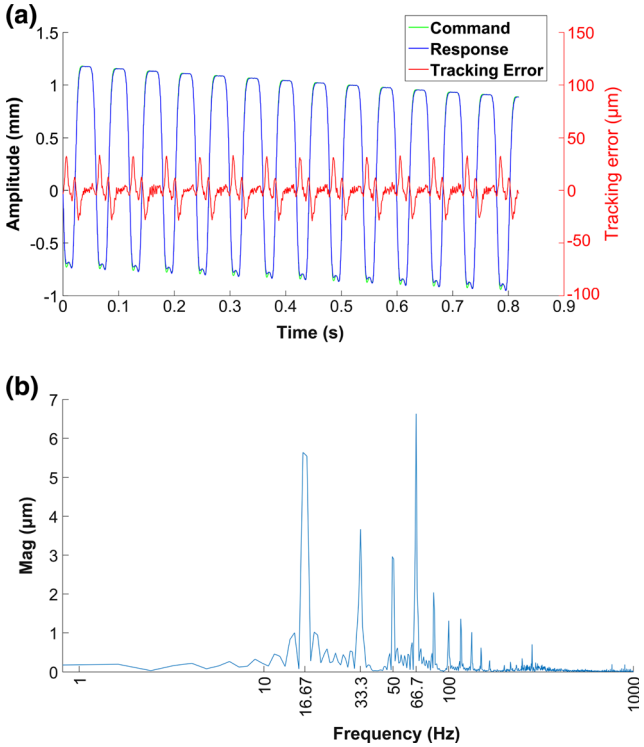

Fig. 10 Motion tracking of LFTS during the diamond turning of the periphery zone of the PAL surface. The spindle speed was set to be 1000 rpm. **a** The comparison of the recorded motion controlled by LFTS and the command. **b** Frequency spectrum of the tracking error

analyze the frequency spectrum of the tracking error as shown in Fig. 10b. The spectrum component at frequency of 16.67 Hz which is half of the nominal working frequency of LFTS may bring local prism deviation to the PAL. The other spectrum components at higher frequency (e.g., 33.3, 50.0, 66.7 Hz …) mainly accounted for the unwanted deviation of the surface curvature as well as the surface power. The overall tracking error shown in Fig. 10a was calculated to be 12 μm (rms). It is believed that the tracking error can be reduced especially in the interior zone of surface because of the decreased motion amplitude of the diamond tool (see Fig. 9).

Upon the completion of surface machining using LFTS, the PAL was polished with a freeform polisher to remove the diamond turning marks. Due to the rotational asymmetric features of the freeform surface, a flexible lap tool supported by the air chamber was used to achieve the uniform polishing effect across the surface.

5 Results of freeform machining

The physical geometrical characterization of the polished surface was measured by the coordinate measuring machine (QVS-3020, Jiaten Corp) using a small ruby stylus tool with a tip radius of 0.5 mm as shown in Fig. 11a. The measurement range of the device is 300 × 200 × 200 mm covering the entire surface geometry of the PAL. The accuracy of profile measurement within the lens aperture, normally 60 mm in diameter, was 0.5 μm which was verified by testing a standard optical flat sample. The surface of the PAL within the central square zone of 41 × 41 mm was scanned with a lateral scanning step of 1.0 mm in both the x and y directions. The measured coordinates were fit with a set of Zernike basis functions to reconstruct the surface which was then compared with the theoretical design to calculate the minimum shape error via surface tilting and rotation. Figure 11b shows the final surface deviation within a circular aperture of 40 mm in diameter when the minimum shape error was obtained. The shape error was calculated to be 6.7 μm (rms) which was a sum of different error sources such as the tracking error of LFTS, absence of tool radius compensation, over polishing, and the profile measurement accuracy due to the local surface slope. The surface deviation in the peripheral region seemed to be worse than that in the central region mainly due to the tracking error of LFTS suffered from the relatively large motion amplitude.

For the evaluation of the optical characterization of PAL, a spectacle lens inspection system (Rotlex, Class Plus) operating on the Moire interferometer was used to simultaneously measure the distributions of the spherical power and cylindrical power with the accuracy of 0.03 diopter as shown in Fig. 12. The measured spherical power was −1.87 diopter

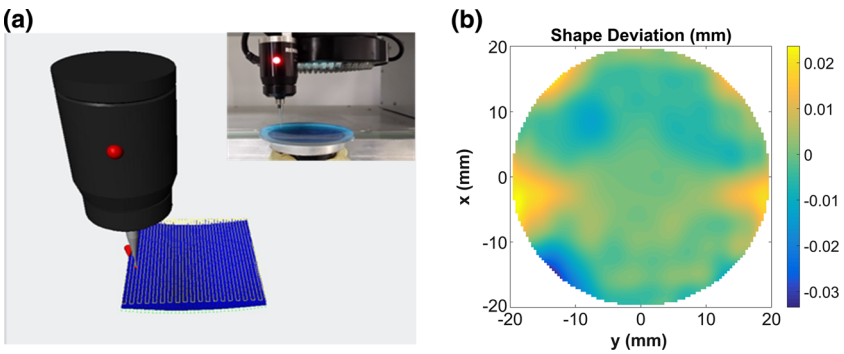

Fig. 11 Geometrical characterization of the polished PAL surface. **a** Surface profile measurement with coordinate measuring machine (41 × 41 mm, 1 mm/step). **b** Shape deviation from the designed freeform surface

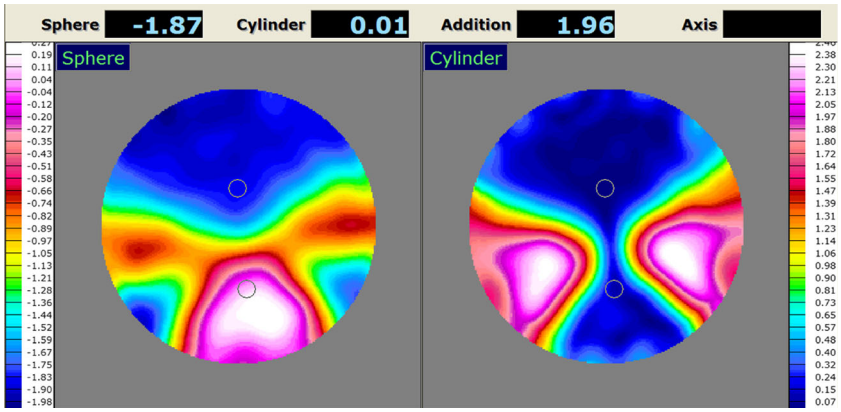

Fig. 12 The measured spherical power and cylinder of the PAL within the lens aperture of 60 mm in diameter

for distant correction with add power of 1.96 diopter matching well with the theoretical design.

The complete process chain from surface machining to polishing of the PAL takes about 5 min and is considered to be feasible and flexible for various design philosophies of the PAL since the diamond tool path can be generated for each design case very quickly. Therefore, the freeform machining based on our LFTS provides an efficient solution to the production of customized PALs which is still out of the capability of traditional molding techniques [2–7].

6 Conclusion

Surface machining of PALs using FTS can be challenging because of the large magnitude of the asymmetric features of the freeform surface. To solve the problem, we developed a prototype of LFTS to control the motion of the diamond tool using the closed loop control system and investigated the fabrication process of the PAL. Both the shape error and the power distributions measured in experiments verified the capability of LFTS for the freeform machining of PAL. We believe that the utilization of LFTS allows for the efficient fabrication of personalized PALs that differ in various design philosophies therefore paving the way for the massive customized production. As part of future investigation, we will may develop an aerostatic guider and replace the rolling guider now employed in LFTS to improve precision of position control accuracy and machining efficiency. The correction cycles to improve the shape of freeform surface after a metrology step will also be included.

Acknowledgment This research is supported by the Natural Science Foundation of Zhejiang Province (LY14F050009, LY14H180007, LY16H120007), Public Interest Science and Technology Program of Wenzhou (G20160033, Y20160438), and the National Natural Science Foundation of China (81300804).

References

1. Sheedy JE (2004) Progressive addition lenses—matching the specific lens to patient needs. Optometry-journal of the American Optometric Association 75(2):83–102. doi:10.1016/S1529-1839(04)70021-4
2. Lochegnies D, Moreau P, Hanriot F, Hugonneaux P (2013) 3D modelling of thermal replication for designing progressive glass moulds. New Journal of Glass and Ceramics 3:34–42. doi:10.4236/njgc.2013.31006
3. Qiu GF, Cui XD (2015) Hyperbolic tangential function-based progressive addition lens design. Appl Opt 54(35):10404–10408. doi:10.1364/AO.54.010404
4. Kong LB, Cheung CF, To S, Wang B, Ho LT (2014) A theoretical and experimental investigation of design and slow tool servo machining of freeform progressive addition lenses (PALs) for optometric applications. Int J Adv Manuf Technol 72(1–4):33–40. doi:10.1007/s00170-012-3901-1
5. Li LK, Raash TW, Yi AY (2013) Simulation and measurement of optical aberrations of injection molded progressive addition lenses. Appl Opt 52(24):6022–6029. doi:10.1364/AO.52.006022
6. Hsu WY, Liu YL, Cheng YC, Su GD (2010) Design and fabrication of the progressive addition lens. Frontiers in Optics. doi:10.1364/FIO.2010.FThU8
7. Hsu WY, Liu YL, Cheng YC, Kuo CH, Chen CC, Su GD (2012) Design, fabrication, and metrology of ultra-precision optical freeform surface for progressive addition lens with B-spline description. Int J Adv Manuf Technol 63(1–4):225–233. doi:10.1007/s00170-012-3901-1
8. Scheiding S, Yi AY, Gebhardt A et al (2011) Freeform manufacturing of a microoptical lens array on a steep curved substrate by use of a voice coil fast tool servo. Opt Express 19(24):23938–23951. doi:10.1364/OE.19.023938
9. Tian FJ, Yin ZQ, Li SY (2015) Fast tool servo diamond turning of optical freeform surfaces for rear-view mirrors. Int J Adv Manuf Technol 80(9–12):1759–1765. doi:10.1007/s00170-015-7152-9
10. Tian FJ, Yin ZQ, Li SY (2016) A novel long rang fast tool servo for diamond turning. Int J Adv Manuf Technol. doi:10.1007/s00170-015-8282-9
11. Zhu ZW, Zhou XQ, Liu ZW, Wang RQ, Zhu L (2014) Development of a piezoelectrically actuated two-degree-of-freedom fast tool servo with decoupled motions for micro-nanomachining. Precis Eng 38(4):809–820. doi:10.1016/j.precisioneng.2014.04.009
12. Rakuff S, Cuttino JF (2009) Design and testing of a long-range, precision fast tool servo system for diamond turning. Precis Eng 33(1):18–25. doi:10.1016/j.precisioneng.2008.03.001
13. Kim HS, Lee KI, Lee KM, Bang YB (2009) Fabrication of free-form surfaces using a long-stroke fast tool servo and

corrective figuring with on-machine measurement. International Journal of Machine Tools & Manufacture 49(12–13):991–997. doi:10.1016/j.ijmachtools.2009.06.011
14. Ludwick SJ, Chargin DA, Calzaretta JA, Trumper DL (1999) Design of a rotary fast tool servo for ophthalmic lens fabrication. Precis Eng 23(4):253–259. doi:10.1016/s0141-6359(99)0017-3
15. Meister DJ, Fisher SW (2008) Progress in the spectacle correction of presbyopia. Part 1: design and development of progressive lenses. Clin Exp Optom 91(3):240–250. doi:10.1111/j.1444-0938.2007.00245.x
16. Winthrop JT (1989) Progressive addition spectacle lens. US Patent 4861153
17. Winthrop JT (1992) Progressive addition spectacle lens. US Patent 313689
18. Yu DP, Wong YS, Hong GS (2011) Optimal selection of machining parameters for fast tool servo diamond turning. Int J Adv Manuf Technol 57(1–4):85–99. doi:10.1007/s00170-011-3280-z